Nanoscale

COMMUNICATION

Accelerating peroxidase mimicking nanozymes using DNA

Biwu Liu and Juewen Liu*

Received 00th January 20xx,
Accepted 00th January 20xx

DOI: 10.1039/x0xx00000x

www.rsc.org/

DNA-capped iron oxide nanoparticles are nearly 10-fold more active as a peroxidase mimic for TMB oxidation compared to the naked nanoparticles. To understand the mechanism, the effect of DNA length and sequence is systematically studied, and other types of polymers are also compared. This rate enhancement is more obvious with longer DNA and in particular, poly-cytosine. Among the various polymer coatings tested, DNA offers the highest rate enhancement. Similar acceleration is also observed with nanoceria. On the other hand, when the positively charged TMB substrate is replaced by the negatively charged ABTS, DNA inhibits oxidation. Therefore, the negatively charged phosphate backbone and bases of DNA can increase TMB binding by the iron oxide nanoparticles and thus facilitating the oxidation reaction in the presence of hydrogen peroxide.

Nanomaterials as enzyme mimics (nanozymes) have received considerable attention recently.[1-3] A wide range of nanomaterials including gold nanoparticles,[4, 5] metal oxides,[6-9] and carbon-based materials[10, 11] have been reported to have oxidase, peroxidase, catalase, and superoxide dismutase like activity. Among these nanozymes, iron oxide nanoparticles (e.g. Fe_3O_4 NPs) are particularly interesting because of their unique magnetic properties and applications in magnetic resonance imaging, drug delivery, and separation.[2] Based on the peroxidase activity of Fe_3O_4 NPs, colorimetric biosensors for H_2O_2 detection have been developed using chromogenic substrates (e.g. 3,3',5,5'-tetramethylbenzidine (TMB), and 2,2'-azino-bis(3-ethylbenzothiazoline-6-sulfonic acid) (ABTS)).[12] When glucose oxidase is combined with Fe_3O_4 NPs, glucose can also be selectively detected.[13] For practical applications and fundamental mechanistic understanding, factors affecting the peroxidase activity need to be fully addressed.[14-17] For example, the surface Fe^{2+} content was found to be vital in its oxidation activity.[6] Prussian blue modified γ-Fe_2O_3 NPs have an elevated surface Fe^{2+} content and thus a higher enzymatic activity.[15] Also, the role of surface charge on substrate oxidation was investigated and electrostatic interaction was found to be crucial for substrate binding.[14] The activity of unmodified NPs is often quite low, and an important challenge in this field is to promote their catalytic activity. We reason this goal might be achieved via understanding the surface chemistry of the reactions.

DNA-functionalized NPs represent an important hybrid material in bionanotechnology.[18-21] Since the seminal work by the Mirkin and Alivisatos groups,[22, 23] a plethora of DNA-NP conjugates have been reported for various applications, such as directed assembly of nanostructures,[24-26] biosensing,[27-30] and drug delivery.[31] DNA functionalization not only improves the colloidal stability of NPs, but also provides additional molecular recognition ability (e.g. aptamers) toward metal ions, small molecules and proteins.[29, 32, 33] DNA-functionalized Fe_3O_4 NPs have been successfully used for detecting arsenate ions,[34] and biomolecules.[35] However, the effect of DNA modification on the intrinsic properties of Fe_3O_4 NPs is less explored. Herein, we communicate that DNA-modified Fe_3O_4 NPs exhibit significantly enhanced peroxidase activity for TMB oxidation compared the bare NPs. Further studies show that both surface charge and DNA base composition are important for modulating the substrate affinity to Fe_3O_4 NPs, and thus the catalytic activity.

Peroxidases catalyse substrate oxidation in the presence of hydrogen peroxide. Fe_3O_4 NPs were first reported to have peroxidase activity in 2007.[6] We characterized our Fe_3O_4 NPs using TEM (Figure S1). The NPs are spherical and have a size range from 20 nm to 50 nm. Slight aggregation was observed attributable to the unmodified surface. We are interested in studying naked NPs without strong capping ligands, so that the surface property can be better controlled. No obvious light absorption features were observed using UV-vis spectroscopy in the visible region from 400 to 800 nm (Figure S2). At low NP concentrations used in this study, this low background absorption does not interfere with visual observation of color change from chromogenic substrates or quantitative spectroscopic measurements.

TMB is a commonly used peroxidase substrate. We next tested oxidation of TMB by Fe_3O_4 NPs. TMB in the reduced state is colorless. DNA and Fe_3O_4 NPs alone do not oxidize TMB (Figure 1a

Department of Chemistry, Waterloo Institute for Nanotechnology, University of Waterloo, Waterloo, Ontario, N2L 3G1, Canada
E-mail: liujw@uwaterloo.ca; Fax: +1 519 746 0435; Tel: +1 519 888 4567 ext. 38919

†.Electronic Supplementary Information (ESI) available: Methods, TEM, UV-vis and DLS data. See DOI: 10.1039/x0xx00000x

and Figure S2). In the presence of unmodified Fe_3O_4 NPs, TMB was slowly oxidized by H_2O_2, producing a moderate blue colour after 15 min (Figure 1a). Interestingly, a strong blue color appeared when DNA was added to the reaction mixture. The change of absorbance at 652 nm is around 8-fold higher with DNA than that with only the unmodified Fe_3O_4 NPs (Figure 1b). Therefore, DNA has promoted the activity of Fe_3O_4 NPs as a peroxidase. To test the generality of this observation, we then employed Fe_2O_3 NPs. Fe_2O_3 was reported to have a lower peroxidase activity (likely due to the lack of Fe^{2+} on the surface),[6] and DNA also induced faster colour change (Figure S3). This significant rate enhancement has prompted us to conduct more research for a better understanding.

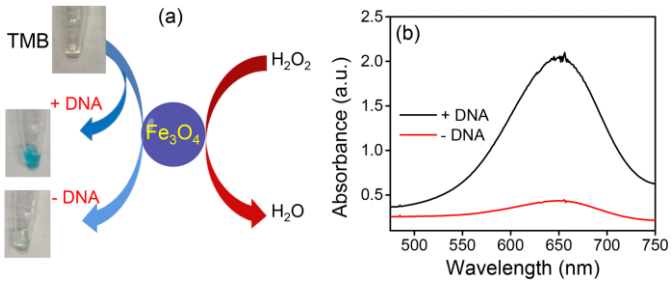

Figure 1. (a) Accelerated oxidation of TMB using the C_{30} DNA-modified Fe_3O_4 NPs as a peroxidase mimic. The photographs of the reaction substrate and product are shown. (b) UV-vis spectra of the reaction products with and without DNA after 15 min reaction.

Our previous work has indicated that DNA is tightly adsorbed by Fe_3O_4 NPs mainly via the phosphate backbone of DNA at neutral pH.[34] From ζ-potential measurement, Fe_3O_4 NPs carry a negative charge at pH 7.6 and a positively charge at pH 4 (Table S2). Our TMB oxidation experiment was carried out at pH 4, and thus electrostatic interaction might also contribute to DNA adsorption. To evaluate the effect of DNA on the peroxidase property of Fe_3O_4 NPs, we first tested the kinetics of TMB oxidation as a function of DNA sequence. Fe_3O_4 NPs were incubated with 15-mer homo DNAs (A_{15}, T_{15}, C_{15}, G_{15}) at pH 4 (acetate buffer, 10 mM) for 10 min, followed by adding the substrate TMB. In the absence of H_2O_2, oxidation of TMB was slow and the added DNA did not alter the reaction (Figure S2). After adding H_2O_2, the reaction showed a DNA sequence dependent kinetics (Figure 2a). The order of reaction kinetics is: C > G > T > A > No DNA. The initial rate of the C_{15}-Fe_3O_4 NP conjugate is 9 times faster than that of unmodified Fe_3O_4 NPs, showing a significant enhancement effect. While we reported the major binding between DNA and Fe_3O_4 NPs are from the phosphate backbone, the secondary structure of homo DNAs may cause different interactions. C_{15} was also found to be the most effective probe used for arsenate detection.[34] The pK_a of cytosine is 4.5, and a large fraction of the base at pH 4 is protonated, which may assist charge neutralization on the particle surface and reduce repulsion among DNA, allowing the packing of more DNA and accelerate the oxidation activity.

Next, we tested the effect of DNA length on the rate enhancement. By fixing the total concentration of nucleosides, we used poly C_n (n = 5, 10, 15, and 30) to modify Fe_3O_4 NPs (e.g. the concentration of C_5 is six times higher than that of C_{30}). The initial rate exhibits a DNA length-dependent increase (Figure 2b). Poly C_{30}, the longest DNA tested here, shows the largest enhancement, even though its molar concentration is the lowest. Longer DNAs have higher affinity with the Fe_3O_4 NPs due to the presence of more binding sites (e.g. polyvalent binding effect). This experiment strongly indicates that DNA adsorption affinity is crucial for activity enhancement. The fact that longer DNA provided higher activity suggests that the activity enhancement is from surface bound DNA.

We further examined the effect of DNA concentration. As shown in Figure 2c, higher DNA concentration induced faster TMB oxidation. When the concentration is higher than 500 nM, the enhancement is less significant, likely due to surface saturation (Figure S4). This experiment also indicates that it is the surface adsorbed DNA instead of free DNA in this system to increase the peroxidase activity of Fe_3O_4 NPs.

Since the peroxidase activity of Fe_3O_4 NPs is pH-dependent[6] and pH may affect DNA adsorption, the effect of pH on the TMB oxidation was also tested. For the free Fe_3O_4 NPs (green bars, Figure 2d), the reaction is more effective at lower pH (e.g. pH 4) as reported in the literature. The presence of DNA does not alter the pH-dependent activity trend, but has enhanced the rate at each pH. It is interesting to note that at pH 6, the color change of TMB with DNA modified NPs is comparable to that at pH 4 with the unmodified Fe_3O_4 NPs. Attaching DNA can expand the application of Fe_3O_4 NPs over a broader pH range. The kinetic data of these reactions are shown in Figure S5.

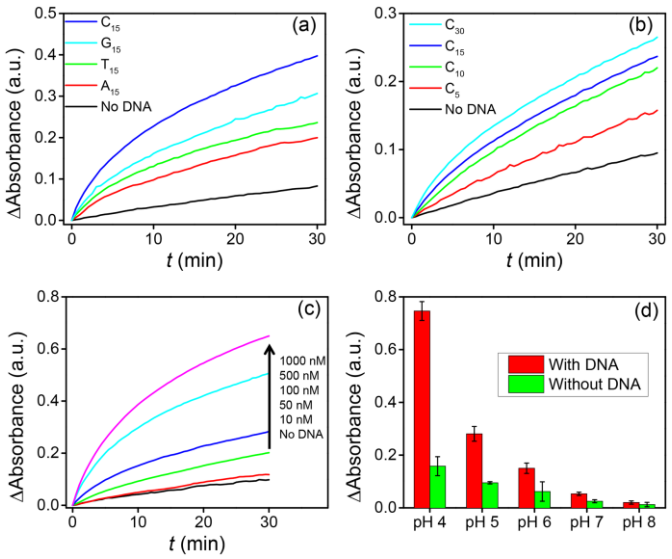

Figure 2. Effects of DNA (a) sequence, (b) length, (c) concentration on the kinetics of TMB oxidation catalysed by DNA modified Fe_3O_4 NPs. (d) The variation of absorbance at 652 nm as a function of pH values in the presence and absence of DNA. The error bars represent the standard deviation from three measurements.

Using polymer coatings to modulate nanozymes activity was also reported in a few other systems.[14] In those examples, electrostatic interaction between Fe_3O_4 NPs and the substrates (TMB and ABTS) was found to be important for the enzyme activity. If TMB (positively charged) was used as a substrate, more negatively charged particles showed higher k_{cat} values.[14] In another example,

DNA from PCR products was reported to inhibit o-phenylenediamine oxidation, as the electrostatic interaction between the positively charged substrate and the negatively charged Fe_3O_4 NP surface is blocked by free DNA in solution and on particle surface.[36] To understand the mechanism here, we first studied whether H_2O_2 and TMB can compete with DNA adsorption. We recently reported that H_2O_2 can efficiently displace DNA adsorbed by CeO_2 NPs due to the strong affinity between H_2O_2 and CeO_2.[37] However, H_2O_2 only inhibited DNA adsorption by Fe_3O_4 NPs at a very high concentration (1 M) and no adsorption inhibition was observed at our experimental conditions (Figure 3a). TMB did not block and even slightly facilitated DNA adsorption onto Fe_3O_4 NPs (Figure 3b). Second, we examined the integrity of DNA by gel electrophoresis. One concern is that DNA might be degraded in the presence of H_2O_2 and iron species (e.g. via the Fenton chemistry). The control group (Fe^{2+}/H_2O_2, lane 6, Figure 3c) indeed shows that the fluorophore tag on DNA (6-carboxyfluorescein, FAM) might be damaged due to generated hydroxyl free radicals indicated by the weak fluorescence intensity. However, DNA on the Fe_3O_4 NPs surface was not cleaved and the fluorophore was not damaged at our experimental conditions (lane 5, Figure 3c). Combined with fluorescence-based results, DNA remained intact on the surface during and after the peroxidase reaction.

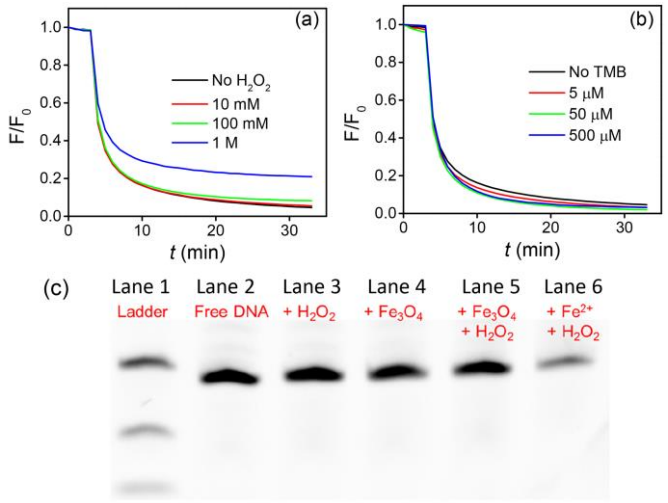

Figure 3. Kinetics of Alexa-DNA (50 nM) adsorption onto Fe_3O_4 NPs (25 μg/mL) at pH 4 (acetate buffer, 10 mM) in the presence of varying concentrations of (a) H_2O_2 and (b) TMB. The lack of obvious kinetic changes indicate that H_2O_2 and TMB do not inhibit DNA adsorption. (c) Gel image of DNA-Fe_3O_4 treated with H_2O_2. Lane 1 is a DNA ladder with FAM-A_5, FAM-A_{15} and FAM-A_{30}. Lane 2 is an untreated FAM-labeled 24 mer DNA. Lane 3-6 are the FAM DNA treated with various chemicals as indicated in the lanes. Acetate buffer (pH 4, 10 mM) was used for all samples. FAM-24 mer DNA (200 nM) was incubated with Fe_3O_4 NPs (25 μg/mL) or Fe^{2+} (50 μM) and H_2O_2 (10 mM) was added if necessary.

One possibility is that DNA facilitates the adsorption of TMB by Fe_3O_4 NPs. With two amino groups, the nonoxidized TMB has a pK_a of ~ 4.2 and is partially positive charged at pH 4 (Figure 4b). This may explain its affinity for DNA. If this hypothesis is true, the activity of Fe_3O_4 NPs should decrease when a negatively charged substrate is used. To test this hypothesis, we then employed another peroxidase substrate, ABTS. ABTS is negative charged due to the dual sulfate anions (Figure 4b). As shown in Figure 4a, after adding H_2O_2 (10 min), ABTS was oxidized by the unmodified Fe_3O_4 NPs but not by the DNA-modified Fe_3O_4 NPs. DNA modification alters the surface charge of Fe_3O_4 NPs from positive to negative (Table S2). The charge repulsion between ABTS and DNA surface inhibits the oxidation reaction. To further prove the charge repulsion mechanism, we monitored the oxidation of ABTS at different ionic strengths. In the absence of DNA, increasing NaCl concentration slightly inhibited TMB oxidation. In the presence of DNA, we found that the enzymatic performance was gradually recovered by increasing NaCl concentration to screen charge repulsion and the activity is even higher than unmodified Fe_3O_4 NPs without additional NaCl (Figure 4c,d).

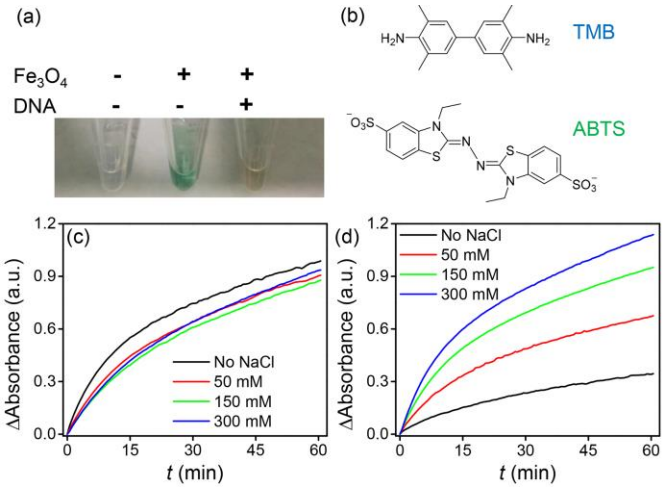

Figure 4. Oxidation of ABTS (1 mM) in the presence of Fe_3O_4 NPs (50 μg/mL) at pH 4. (a) A photograph showing oxidation of ABTS producing a green colour. The reaction is inhibited by DNA modification. (b) Chemical structures of TMB and ABTS. Kinetics of ABTS oxidation at various NaCl concentrations catalysed by (c) bare Fe_3O_4 NPs and (d) DNA-capped Fe_3O_4 NPs, respectively. The absorbance at 420 nm was monitored.

Aside from the negatively charged backbone, DNA can also provide hydrogen bonding, π-π interactions via DNA bases. To test if DNA bases are involved in substrate binding, we compared DNA with other negatively charged polymers for coating Fe_3O_4 NPs. Polyacrylic acid (PAA) and polystyrene sulfonate (PSS) were respectively used to modify Fe_3O_4 NPs. The surface charge alternation at pH 4 was confirmed by ζ-potential measurement and all modified Fe_3O_4 NPs exhibit similar negative charge values (Table S2). Compared to unmodified Fe_3O_4 NPs, negatively charged NPs all enhanced the activity and DNA modification provides the highest enhancement, followed by PSS and PAA (Figure 5a). DNA-modified Fe_2O_3 NPs also exhibited higher activity than PSS modified ones. (Figure S3b). To further emphasize the importance of DNA bases, we compared Fe_3O_4 NPs modified by phosphate, guanosine monophosphate (GMP), and G_{15} (Figure 5b). Phosphate also changes the surface charge of Fe_3O_4 NPs to be negative (Table S2); however, the activity increase is minimal. As expected, GMP-modified Fe_3O_4 NPs facilitate TMB oxidation, confirming the role the

DNA bases. The further increased activity by G_{15} functionalization is consistent with our observation that the enhancement is DNA length-dependent (Figure 2b). We propose that DNA bases also facilitate the substrate binding via hydrogen bonding with the amino groups of TMB, and/or the nucleobase interacting with the benzene rings of TMB via π- π stacking.

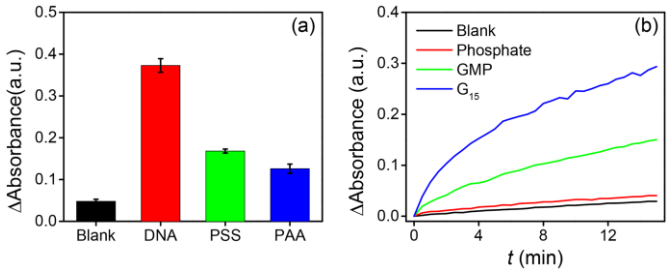

Figure 5. Comparison of the peroxidase activity of DNA-Fe_3O_4 NPs with (a) various negatively charged polymers coated Fe_3O_4 NPs and (b) phosphate and GMP modified Fe_3O_4 NPs. The error bars represent standard deviation from three independent measurements.

Now that we have changed the polymer coating and substrate, we finally also tested a different type of NP, CeO_2. We previously reported that the oxidase activity of CeO_2 is inhibited by adsorbed DNA for oxidation of TMB.[38] However, the peroxidase activity of CeO_2 is actually enhanced by DNA modification (Figure S6). This might be attributed to that TMB needs to be directly adsorbed by CeO_2 to be oxidized in the absence of H_2O_2 (i.e. CeO_2 surface works as an oxidizing agent).[39] However, in the presence of H_2O_2, CeO_2 can mediate the oxidation at a distance from the surface. As an oxidase, the TMB substrate need to get onto the particle surface since the oxidizing agent is the particle surface. As a peroxidase, the actual oxidizing agent is derived from H_2O_2 (e.g. reactive oxygen species), which can diffuse near the particle surface. The activity of Fe_3O_4 NPs we studied here is the peroxidase activity. In this case, the surface is likely to react with H_2O_2 and then the reactive oxygen species produced in this process is used to oxidize TMB. H_2O_2 is a much smaller molecule and DNA does not block its access to the Fe_3O_4 NPs.

In summary, we observed a significant rate enhancement brought by DNA for the peroxidase activity of Fe_3O_4 NPs for TMB oxidation. Such a rate enhancement will make such a nanozyme a better material for biosensor development and catalysis. Starting from this observation, we investigated the effect of DNA adsorption on enhancing the peroxidase-like activity of Fe_3O_4 NPs. DNA/Fe_3O_4 forms a stable hybrid material, and neither H_2O_2 nor TMB can displace DNA from the particle surface under our experimental conditions. Among all the tested anionic polymers, DNA affords the highest rate enhancement. This is attributed to both electrostatic attraction and aromatic stacking with the substrate TMB. The hypothesis is further supported by using a negative charged substrate ABTS and with CeO_2 NPs. The insight from this work will be useful for further rational improving nanozyme activity via surface modification.

Funding for this work is from the University of Waterloo, the Canadian Foundation for Innovation, the NSERC of Canada, and the Early Researcher Award from the Ontario Ministry of Research and Innovation.

Notes and references

1. Y. Lin, J. Ren and X. Qu, *Acc. Chem. Res.*, 2014, **47**, 1097-1105.
2. H. Wei and E. Wang, *Chem. Soc. Rev.*, 2013, **42**, 6060-6093.
3. I. Celardo, J. Z. Pedersen, E. Traversa and L. Ghibelli, *Nanoscale*, 2011, **3**, 1411-1420.
4. M. Comotti, C. Della Pina, R. Matarrese and M. Rossi, *Angew. Chem. Int. Ed.*, 2004, **43**, 5812-5815.
5. W. Luo, C. Zhu, S. Su, D. Li, Y. He, Q. Huang and C. Fan, *ACS Nano*, 2010, **4**, 7451-7458.
6. L. Gao, J. Zhuang, L. Nie, J. Zhang, Y. Zhang, N. Gu, T. Wang, J. Feng, D. Yang, S. Perrett and X. Yan, *Nat. Nanotechnol.*, 2007, **2**, 577-583.
7. A. Asati, S. Santra, C. Kaittanis, S. Nath and J. M. Perez, *Angew. Chem. Int. Ed.*, 2009, **48**, 2308-2312.
8. J. Dong, L. Song, J.-J. Yin, W. He, Y. Wu, N. Gu and Y. Zhang, *ACS Appl. Mater. Interfaces*, 2014, **6**, 1959-1970.
9. R. Ragg, F. Natalio, M. N. Tahir, H. Janssen, A. Kashyap, D. Strand, S. Strand and W. Tremel, *ACS Nano*, 2014, **8**, 5182-5189.
10. Y. Song, K. Qu, C. Zhao, J. Ren and X. Qu, *Adv. Mater.*, 2010, **22**, 2206-2210.
11. Y. Song, X. Wang, C. Zhao, K. Qu, J. Ren and X. Qu, *Chem. – Eur. J.*, 2010, **16**, 3617-3621.
12. H. Wei and E. Wang, *Anal. Chem.*, 2008, **80**, 2250-2254.
13. Y.-l. Dong, H.-g. Zhang, Z. U. Rahman, L. Su, X.-j. Chen, J. Hu and X.-g. Chen, *Nanoscale*, 2012, **4**, 3969-3976.
14. F. Yu, Y. Huang, A. J. Cole and V. C. Yang, *Biomaterials*, 2009, **30**, 4716-4722.
15. X.-Q. Zhang, S.-W. Gong, Y. Zhang, T. Yang, C.-Y. Wang and N. Gu, *J. Mater. Chem.*, 2010, **20**, 5110-5116.
16. S. Liu, F. Lu, R. Xing and J.-J. Zhu, *Chem. – Eur. J.*, 2011, **17**, 620-625.
17. K. N. Chaudhari, N. K. Chaudhari and J.-S. Yu, *Catal. Sci. Technol.*, 2012, **2**, 119-124.
18. J. I. Cutler, E. Auyeung and C. A. Mirkin, *J. Am. Chem. Soc.*, 2012, **134**, 1376-1391.
19. K. Saha, S. S. Agasti, C. Kim, X. Li and V. M. Rotello, *Chem. Rev.*, 2012, **112**, 2739-2779.
20. O. I. Wilner and I. Willner, *Chem. Rev.*, 2012, **112**, 2528-2556.
21. V. Tjong, L. Tang, S. Zauscher and A. Chilkoti, *Chem. Soc. Rev.*, 2014, **43**, 1612-1626.
22. C. A. Mirkin, R. L. Letsinger, R. C. Mucic and J. J. Storhoff, *Nature*, 1996, **382**, 607-609.
23. A. P. Alivisatos, K. P. Johnsson, X. Peng, T. E. Wilson, C. J. Loweth, M. P. Bruchez and P. G. Schultz, *Nature*, 1996, **382**, 609-611.
24. J. J. Storhoff and C. A. Mirkin, *Chem. Rev.*, 1999, **99**, 1849-1862.
25. Y. Lu and J. Liu, *Acc. Chem. Res.*, 2007, **40**, 315-323.
26. E. Katz and I. Willner, *Angew. Chem. Int. Ed.*, 2004, **43**, 6042-6108.
27. C.-H. Lu, H.-H. Yang, C.-L. Zhu, X. Chen and G.-N. Chen, *Angew. Chem. Int. Ed.*, 2009, **48**, 4785-4787.

28. H. Wang, R. Yang, L. Yang and W. Tan, *ACS Nano*, 2009, **3**, 2451-2460.
29. J. Liu, Z. Cao and Y. Lu, *Chem. Rev.*, 2009, **109**, 1948-1998.
30. N. L. Rosi and C. A. Mirkin, *Chem. Rev.*, 2005, **105**, 1547-1562.
31. D. A. Giljohann, D. S. Seferos, W. L. Daniel, M. D. Massich, P. C. Patel and C. A. Mirkin, *Angew. Chem. Int. Ed.*, 2010, **49**, 3280-3294.
32. D. Li, S. Song and C. Fan, *Acc. Chem. Res.*, 2010, **43**, 631-641.
33. W. Tan, M. J. Donovan and J. Jiang, *Chem. Rev.*, 2013, **113**, 2842-2862.
34. B. Liu and J. Liu, *Chem. Commun.*, 2014, **50**, 8568-8570.
35. C. Song, G.-Y. Wang and D.-M. Kong, *Biosens. Bioelectron.*, 2015, **68**, 239-244.
36. K. S. Park, M. I. Kim, D.-Y. Cho and H. G. Park, *Small*, 2011, **7**, 1521-1525.
37. B. Liu, Z. Sun, P.-J. J. Huang and J. Liu, *J. Am. Chem. Soc.*, 2015, **137**, 1290-1295.
38. R. Pautler, E. Y. Kelly, P.-J. J. Huang, J. Cao, B. Liu and J. Liu, *ACS Appl. Mater. Interfaces*, 2013, **5**, 6820-6825.
39. Y. Peng, X. Chen, G. Yi and Z. Gao, *Chem. Commun.*, 2011, **47**, 2916-2918.